Measurement 176 (2021) 109139

Contents lists available at ScienceDirect

Measurement

journal homepage: www.elsevier.com/locate/measurement

Multiple fading factors-based strong tracking variational Bayesian adaptive Kalman filter

Cheng Pan [a,b], Jingxiang Gao [a,b,*], Zengke Li [a,b], Nijia Qian [a,b], Fangchao Li [a,b,c]

[a] MNR Key Laboratory of Land Environment and Disaster Monitoring, China University of Mining and Technology, Xuzhou 221116, China
[b] School of Environmental Science and Spatial Informatics, China University of Mining and Technology, Xuzhou 221116, China
[c] Nottingham Geospatial Institute, University of Nottingham, Nottingham NG7 2RD, United Kingdom

ARTICLE INFO

Keywords:
Strong tracking theory
Multiple fading factors
Noise covariance matrix
Variational Bayesian
Adaptive Kalman filter

ABSTRACT

If the system model or the statistical characteristics of noise are inaccurate, the past measurements will directly affect the accuracy of current state estimation or even lead to filtering divergence. To overcome above difficulties, a multiple fading factors-based strong tracking variational Bayesian adaptive Kalman filter is proposed. Firstly, the inverse Wishart distribution is adopted to model the measurement noise covariance matrix. Secondly, the remodified measurement noise covariance matrix and the innovation covariance matrix estimated by exponential weighting method are employed to construct the scalar fading factor. Next, the multiple fading factors are calculated to correct the predicted error covariance matrix. Finally, the local optimal estimations of measurement noise covariance matrix and state are obtained by variational Bayesian approach. The target tracking simulations verify that the proposed algorithm has better tracking ability for the predicted error covariance matrix and the measurement noise covariance matrix compared with the existing filters.

1. Introduction

For the linear Gaussian state space model whose observation noise and system noise are stationary, the Kalman filter (KF) is a recursive optimal algorithm that employs the minimum mean square error (MMSE) as the estimation criterion and has been widely used in parameter estimation [1,2]. The KF adopts the estimated state vector at previous moment and the measurements at current moment to obtain the current state, which is essentially a process of continuous prediction and correction [3], and it does not need to store a large amount of historical observation data. Due to its excellent parameter estimation performance, the KF has been widely used in various dynamic systems, such as target location and tracking, fault diagnosis and detection, navigation and guidance, risk index assessment and so on [4–8].

However, in practical applications, the noise statistical characteristics of the state space model are not always stationary [9–13]. The time-varying process noise covariance matrix (PNCM) and measurement noise covariance matrix (MNCM) usually affect the accuracy of the prior information obtained from noise statistics, and the wrong prior information will cause a large number of estimation errors or even filtering divergence [14,15], accordingly diminish the filtering performance. Aiming at these problems, scholars put forward numbers of adaptive Kalman filters (AKF), e.g., innovation-based AKF (IAKF), fading AKF (FAKF), variational Bayesian-based AKF (VBAKF), strong tracking-based variational Bayesian AKF (ST-VBAKF) and so on [16–19]. The IAKF solves the problem of imperfect prior information through a filtering learning process based on an innovative sequence, which has a significant improvement in performance over fixed filters [16]. However, the IAKF requires a fairly large data window to obtain a reliable estimation of the MNCM, which makes it unsuitable for rapidly changing MNCM. The FAKF decreases the weights of current observations by increasing the one-step prediction error covariances. However, the calculation process of the scalar fading factor is more cumbersome and it has the same adjustment ability for each filtering channel, which is not conducive to improve the stability and accuracy of the filter [20]. The VBAKF selects the inverse Wishart prior to model the measurement noise, and it uses the variational Bayesian (VB) approach to obtain the suboptimal estimations of the state vector and the slowly varying MNCM [18]. However, the PNCM is set as a fixed value which is not consistent with reality [21], thus, the filtering performance of VBAKF will decrease due to the inaccurate PNCM. On the basis of VBAKF, Huang et al. [15] proposed a novel variational Bayesian-based adaptive Kalman filter (N-

* Corresponding author at: MNR Key Laboratory of Land Environment and Disaster Monitoring, China University of Mining and Technology, Xuzhou 221116, China.
E-mail address: jxgao@cumt.edu.cn (J. Gao).

https://doi.org/10.1016/j.measurement.2021.109139
Received 2 September 2020; Received in revised form 5 January 2021; Accepted 1 February 2021
Available online 10 February 2021

VBAKF), which can estimate not only MNCM but also predicted error covariance matrix (PECM) in the process of variational iterative recursion, and good results have been achieved in the target tracking problem where both PECM and MNCM are slowly varying. However, the N-VBAKF also has the disadvantages of high computational complexity and time consumption. Tan [19] introduced the suboptimal fading factor into VBAKF and proposed a ST-VBAKF algorithm, which could adaptively track the MNCM in a linear Gaussian system with time-varying noise, and effectively overcome the influence of time-varying PNCM. The convergence speed and accuracy of the results are improved. However, as with FAKF, the scalar fading factor has regulatory limitations in ST-VBAKF.

In complex dynamic systems, the estimation accuracies of state variables represented by diagonal elements of PECM are different. Therefore, conventional FAKF can no longer meet the demand of accuracy since the scalar fading factor has the same ability to adjust the state variables. Zhou et al. [22] proposed an extended Kalman filter (EKF) with multiple suboptimal fading factors, which determined the weights corresponding to the fading factors through prior knowledge, and provided a new idea for the establishment of multiple fading factors. Geng et al. [23] scaled the PECM based on an assumption that the prediction residual vectors follow a chi-square distribution, and proposed a novel AKF with multiple fading factors for GPS/INS integrated navigation. The characteristics of this filter overcome the lack of traditional KF in robust estimation. Furthermore, scholars have designed a variety of multiple fading factors-based filters according to the characteristics of different dynamic systems to make the filters more applicable [24–26].

In order to further improve the performance of ST-VBAKF, a multiple fading factors-based strong tracking variational Bayesian adaptive filter (MST-VBAKF) is proposed. Compared with ST-VBAKF, the improvements of proposed method are reflected in two aspects. Firstly, an exponential weighting method based on fading memory is introduced to improve the utilization weight of current observations, thus the innovation covariance matrix is estimated more accurately. Secondly, the multiple fading factors are employed to promote the tracking ability for PECM and the filter robustness is enhanced. Simulation results show that the estimation accuracy of the new algorithm is better than ST-VBAKF and the other filters.

The rest of this paper is organized as follows. Section 2 formulates the problem and gives the KF solution. Section 3 introduces the formation process of the MST-VBAKF in detail, including the selection of prior distributions for process and measurement noise, the construction of multiple fading factors and the derivation of variational measurement update. Section 4 performs simulations to verify the proposed filtering algorithm, in which the influences of weakening factor and forgetting factor on MST-VBAKF and the robustness of different nominal noise covariance settings are analyzed, respectively, and then the proposed filtering algorithm is compared with the existing filters. Section 5 summarizes the performance of the new algorithm.

2. Problem formulation and KF solution

The state space model of discrete linear stochastic system includes state equation and measurement equation, which is defined as [27,28]

$$\boldsymbol{X}_k = \boldsymbol{F}_{k-1}\boldsymbol{X}_{k-1} + \boldsymbol{w}_{k-1} \tag{1}$$

$$\boldsymbol{L}_k = \boldsymbol{H}_k\boldsymbol{X}_k + \boldsymbol{v}_k \tag{2}$$

where $\boldsymbol{X}_k$ and $\boldsymbol{L}_k$ are the state and measurement vectors, respectively; $\boldsymbol{F}_{k-1}$ is the system transition matrix; $\boldsymbol{H}_k$ is the design matrix; $\boldsymbol{w}_{k-1}$ and $\boldsymbol{v}_k$ are the process and measurement noise vectors, respectively. It should be noted that the initial state vector $\boldsymbol{X}_0$ is assumed to be the Gaussian distribution of mean vector $\widehat{\boldsymbol{X}}_{0|0}$ and covariance matrix $\boldsymbol{P}_{0|0}$. In addition, the statistical information of the noise term satisfies the following conditions [26]:

$$\mathrm{E}(\boldsymbol{w}_k) = \boldsymbol{0},\ \mathrm{Cov}(\boldsymbol{w}_k, \boldsymbol{w}_j^{\mathrm{T}}) = \boldsymbol{Q}_k\delta_{kj} \tag{3}$$

$$\mathrm{E}(\boldsymbol{v}_k) = \boldsymbol{0},\ \mathrm{Cov}(\boldsymbol{v}_k, \boldsymbol{v}_j^{\mathrm{T}}) = \boldsymbol{R}_k\delta_{kj} \tag{4}$$

$$\mathrm{Cov}(\boldsymbol{w}_k, \boldsymbol{v}_j^{\mathrm{T}}) = \boldsymbol{0} \tag{5}$$

where $\boldsymbol{Q}_k$ and $\boldsymbol{R}_k$ are the true process and measurement noise covariance matrices, respectively, which are positive definite symmetric matrices; δ_{kj} represents the Kronecker-delta function equal to the unit quantity at $k = j$ and zero elsewhere [29].

For the linear Gaussian state space model like Equations (1) and (2), the filtering recursive process can be divided into two steps: the prediction and the update [3]. The prediction process is mainly to use the time update equation to establish the priori estimation of current state, that is, the estimations of current state vector and the error covariance matrix are calculated forward in time according to the posterior estimation of the previous state. According to the principle of least squares, the predicted state vector $\widehat{\boldsymbol{X}}_{k|k-1}$ and PECM $\boldsymbol{P}_{k|k-1}$ of KF at time k are formulated as [30,31]

$$\widehat{\boldsymbol{X}}_{k|k-1} = \boldsymbol{F}_{k-1}\widehat{\boldsymbol{X}}_{\mathrm{k}\text{ - }1|k-1} \tag{6}$$

$$\boldsymbol{P}_{k|k-1} = \boldsymbol{F}_{k-1}\boldsymbol{P}_{k-1|k-1}\boldsymbol{F}_{k-1}^{\mathrm{T}} + \widetilde{\boldsymbol{Q}}_{k-1} \tag{7}$$

where $\widetilde{\boldsymbol{Q}}_{k-1}$ denotes the nominal PNCM. The measurement update equation is employed to acquire an improved posterior estimation of the current state based on the prior estimation of the prediction process and the current measurements. The estimated state vector $\widehat{\boldsymbol{X}}_{k|k}$ and error covariance matrix $\boldsymbol{P}_{k|k}$ are given by [31]

$$\boldsymbol{K}_k = \boldsymbol{P}_{k|k-1}\boldsymbol{H}_k^{\mathrm{T}}\left(\boldsymbol{H}_k\boldsymbol{P}_{k|k-1}\boldsymbol{H}_k^{\mathrm{T}} + \widetilde{\boldsymbol{R}}_k\right)^{-1} \tag{8}$$

$$\widehat{\boldsymbol{X}}_{k|k} = \widehat{\boldsymbol{X}}_{k|k-1} + \boldsymbol{K}_k\left(\boldsymbol{L}_k - \boldsymbol{H}_K\widehat{\boldsymbol{X}}_{k|k-1}\right) \tag{9}$$

$$\boldsymbol{P}_{k|k} = (\boldsymbol{I} - \boldsymbol{K}_k\boldsymbol{H}_k)\boldsymbol{P}_{k|k-1} \tag{10}$$

where $\boldsymbol{K}_k$ is the filtering gain matrix; $\widetilde{\boldsymbol{R}}_k$ is the nominal MNCM; $\boldsymbol{I}$ denotes the identity matrix.

In some practical applications, especially for autonomous vehicle navigation and positioning system, the system noise statistics may not reflect the actual noise statistics on the trajectory [11], that is, $\widetilde{\boldsymbol{Q}}_{k-1}$ and $\widetilde{\boldsymbol{R}}_k$ may not be accurate since it is difficult to carry out the high-fidelity simulation for operating environment. According to Equations (7) and (8), the inaccurate PNCM and MNCM will have a terrible effect on the accuracy of KF.

3. Strong tracking variational Bayesian adaptive Kalman filter based on multiple fading factors

In this section, the multiple fading factors are introduced into VBAKF and a novel filtering method named MST-VBAKF is proposed, which can adjust the PECM $\boldsymbol{P}_{k|k-1}$ and inaccurate MNCM $\widetilde{\boldsymbol{R}}_k$ simultaneously. The selection of prior distribution, the construction of multiple fading factors and the variational measurement update process of MST-VBAKF are introduced in detail, respectively.

3.1. Selection of prior distribution

It can be seen from Beal's proof [32] that if a suitable prior distribution of the parameter to be estimated is selected in the conjugate-exponential (CE) family, the new approximated distribution has the same form as the prior distribution but some parameters are changed. In view of the prior distribution, the expressions of the relevant parameters of the new distribution can be easily obtained. Therefore, in Bayesian

theory, the inverse Wishart distribution is usually selected as the conjugate prior for the covariance matrix of the Gaussian distribution with known mean. The prior distribution of the MNCM $\boldsymbol{R}_k$ based on inverse Wishart probability density function (PDF) can be described as [15]:

$$p(\boldsymbol{R}_k|\boldsymbol{L}_{1:k-1}) = \mathrm{IW}(\boldsymbol{R}_k;\ \widehat{v}_{k|k-1},\ \widehat{\boldsymbol{V}}_{k|k-1}) \tag{11}$$

$$\mathrm{IW}(\boldsymbol{R}_k;\ \widehat{v}_{k|k-1},\ \widehat{\boldsymbol{V}}_{k|k-1}) = \frac{\left|\widehat{\boldsymbol{V}}_{k|k-1}\right|^{\frac{\widehat{v}_{k|k-1}}{2}} |\boldsymbol{R}_k|^{-\frac{\left(\widehat{v}_{k|k-1}+d+1\right)}{2}} \exp\{-\frac{1}{2}\mathrm{tr}[\widehat{\boldsymbol{V}}_{k|k-1}\boldsymbol{R}_k^{-1}]\}}{2^{\frac{\widehat{v}_{k|k-1}d}{2}}\Gamma_d(\frac{\widehat{v}_{k|k-1}}{2})} \tag{12}$$

where $\mathrm{IW}(\cdot)$ represents the inverse Wishart PDF; $\widehat{v}_{k|k-1}$ is the degree of freedom parameter; $\widehat{\boldsymbol{V}}_{k|k-1}$ is the inverse scale matrix; d is the dimension of $\boldsymbol{R}_k$; $\Gamma_d(\cdot)$ denotes multiple gamma function; $\mathrm{tr}[\cdot]$ denotes the trace of the matrix. In addition, if $\boldsymbol{R}_k \sim \mathrm{IW}(\boldsymbol{R}_k;\ \widehat{v}_{k|k-1},\ \widehat{\boldsymbol{V}}_{k|k-1})$ and $\widehat{v}_{k|k-1} > d+1$, then $\mathrm{E}(\boldsymbol{R}_k^{-1}) = (\widehat{v}_{k|k-1} - d - 1)\widehat{\boldsymbol{V}}_{k|k-1}^{-1}$.

Assuming that the prior distribution of the joint PDF $p(\boldsymbol{X}_k,\ \boldsymbol{R}_k|\boldsymbol{L}_{1:k-1})$ of the state vector and the MNCM is the product of the Gaussian distribution $p(\boldsymbol{X}_k|\boldsymbol{L}_{1:k-1})$ and the inverse Wishart distribution $p(\boldsymbol{R}_k|\boldsymbol{L}_{1:k-1})$, the prediction process can be defined as

$$p(\boldsymbol{X}_k,\ \boldsymbol{R}_k|\boldsymbol{L}_{1:k-1}) = \mathrm{N}(\boldsymbol{X}_{k-1};\ \widehat{\boldsymbol{X}}_{k|k-1},\ \boldsymbol{P}_{k|k-1})\mathrm{IW}(\boldsymbol{R}_k;\ \widehat{v}_{k|k-1},\ \widehat{\boldsymbol{V}}_{k|k-1}) \tag{13}$$

where $\mathrm{N}(\cdot)$ represents the Gaussian PDF; In order to ensure that the prior distribution $p(\boldsymbol{R}_k|\boldsymbol{L}_{1:k-1})$ follows the inverse Wishart distribution, the one-step predicted results of the distribution parameter $\widehat{v}_{k|k-1}$ and $\widehat{\boldsymbol{V}}_{k|k-1}$ are modified by introducing the change factor ρ as follows [33]:

$$\widehat{v}_{k|k-1} = \rho(\widehat{v}_{k-1|k-1} - d - 1) + d + 1 \tag{14}$$

$$\widehat{\boldsymbol{V}}_{k|k-1} = \rho\widehat{\boldsymbol{V}}_{k-1|k-1} \tag{15}$$

where the changing factor $\rho \in (0,\ 1]$. When $k = 1$, $\widehat{v}_{0|0} = \tau + d + 1$ and $\widehat{\boldsymbol{V}}_{0|0} = \tau\widetilde{\boldsymbol{R}}$. In this paper, $\tau = 3$. Accordingly, the time-varying MNCM will be changed with a certain probability distribution which make posteriori and prior PDFs have the same form.

3.2. Construction of multiple fading factors

Due to the memory of KF, the PECM $\boldsymbol{P}_{k|k-1}$ of state vector at time k may also contain errors since the PNCM $\boldsymbol{Q}_{k-1}$ is inaccurate. The ST-VBAKF equates the system uncertainty to the filtering estimation error. By introducing the single fading factor to adjust the PECM $\boldsymbol{P}_{k|k-1}$, the filtering accuracy is improved. In practical applications [34], however, the estimation accuracy of each state component may be different, and the influence of system uncertainty on the diagonal elements of PECM is different too, so that the application of single fading factor is limited.

In order to weaken the influence of inaccurate $\boldsymbol{P}_{k|k-1}$ on the estimation accuracy, make each filtering channel have different adjustment capability, and further improve the filtering performance when model parameters are unknown or abrupt, multiple suboptimal fading factors are given in this paper, whose matrix form is

$$\boldsymbol{\Lambda}_k = \mathrm{diag}(\lambda_{1,k}, \lambda_{2,k}, \ldots, \lambda_{n,k}) \tag{16}$$

$$\lambda_{i,k} = \mu_i c_k,\ i = 1, \cdots, n \tag{17}$$

where n is the dimension of $\boldsymbol{P}_{k-1|k-1}$; c_k is the scalar fading factor at time k, which is calculated by conventional FAKF algorithm. μ_i represents the weight of the fading factor corresponding to the *ith* state component, which can be determined by prior knowledge of the system. When the prior knowledge is unavailable, multiple fading factors can be reduced to single fading factor, namely $\mu_i = 1,\ i = 1, \cdots, n$.

According to the strong tracking theory, c_k is described as the following form [22,26]:

$$c_k = \begin{cases} \widetilde{c}, & \widetilde{c} > 1 \\ 1, & \widetilde{c} \leqslant 1 \end{cases} \quad \widetilde{c} = \mathrm{tr}[\boldsymbol{N}_k] / \sum_{i=1}^{d} \mu_i M_k^{ii} \tag{18}$$

$$\boldsymbol{N}_k = \boldsymbol{\gamma}_k - \boldsymbol{H}_k\boldsymbol{Q}_{k-1}\boldsymbol{H}_k^{\mathrm{T}} - \beta\widehat{\boldsymbol{R}}_k \tag{19}$$

$$\boldsymbol{M}_k = \boldsymbol{H}_k\boldsymbol{F}_{k-1}\boldsymbol{P}_{k-1|k-1}\boldsymbol{F}_{k-1}^{\mathrm{T}}\boldsymbol{H}_k^{\mathrm{T}} \tag{20}$$

where $\boldsymbol{\gamma}_k$ is the covariance matrix of the output residual vector; β is a weakening factor, whose function is to make the estimation result smoother; $\widehat{\boldsymbol{R}}_k$ is the estimated MNCM based on the inverse Wishart distribution.

In general, $\boldsymbol{\gamma}_k$ is obtained by windowing method, which is similar to Sage filter [35]. In this paper, however, an exponential weighting method based on fading memory is adopted. The weighting coefficient is assigned according to the law of negative exponential function, and the recursive formula of $\boldsymbol{\gamma}_k$ at time k is defined as [20]:

$$\boldsymbol{\gamma}_k = \frac{(1-\zeta)\boldsymbol{\xi}_k\boldsymbol{\xi}_k^{\mathrm{T}} + (\zeta - \zeta^k)\boldsymbol{\gamma}_{k-1}}{1-\zeta^k} \tag{21}$$

where $\boldsymbol{\gamma}_0 = 0$; $\boldsymbol{\xi}_k$ is the residual vector; $0.65 \leqslant \zeta \leqslant 0.95$ is the forgetting factor, whose function is to strengthen the influence of the residual sequence and improve the tracking ability of the algorithm.

Fig. 1 shows the construction of multiple fading factors. Since the multiple fading factors $\boldsymbol{\Lambda}_k$ focus on controlling the state estimation error at time $k-1$, accordingly $\boldsymbol{\Lambda}_k$ only act on the estimated state vector covariance matrix $\boldsymbol{P}_{k-1|k-1}$ in Equation (7), namely

$$\widehat{\boldsymbol{P}}_{k|k-1} = \boldsymbol{\Lambda}_k\boldsymbol{F}_{k-1}\boldsymbol{P}_{k-1|k-1}\boldsymbol{F}_{k-1}^{\mathrm{T}} + \widetilde{\boldsymbol{Q}}_{k-1} \tag{22}$$

3.3. Variational measurement update

The VB approach is an approximation method, which adopts a number of known distributions to represent the complicated posterior distribution. In view of the VB statistical theory, the true posterior distribution $p(\boldsymbol{X}_k, \boldsymbol{R}_k|\boldsymbol{L}_{1:k})$ can be approximately expressed as the product of $q(\boldsymbol{X}_k)$ and $q(\boldsymbol{R}_k)$, where $q(\boldsymbol{X}_k)$ follows the Gaussian distribution and $q(\boldsymbol{R}_k)$ follows the inverse Wishart distribution [36]. The Kullback-Leibler divergence (KLD) is introduced to describe how close the approximate distribution is to the real distribution. The divergence function is defined as [36]:

$$\begin{aligned} &\mathrm{KLD}(q(\boldsymbol{X}_k)q(\boldsymbol{R}_k)||\mathrm{p}(\mathbf{X}_k, \mathbf{R}_{k-1}|\mathbf{L}_{1:k})) = \\ &\int q(\boldsymbol{X}_k)q(\boldsymbol{R}_k) \times ln\frac{q(\boldsymbol{X}_k)q(\boldsymbol{R}_k)}{p(\boldsymbol{X}_k, \boldsymbol{R}_{k-1}|\boldsymbol{L}_{1:k})}\mathrm{d}\boldsymbol{X}_k\mathrm{d}\boldsymbol{R}_k \end{aligned} \tag{23}$$

when the KLD in the variational update process is equal to 0, $q(\boldsymbol{X}_k)q(\boldsymbol{R}_k) = p(\boldsymbol{X}_k,\ \boldsymbol{R}_k|\boldsymbol{L}_{1:k})$, then the optimal estimation of the parameter can be obtained.

According to Beal's proof [32], the logarithmic expression of the

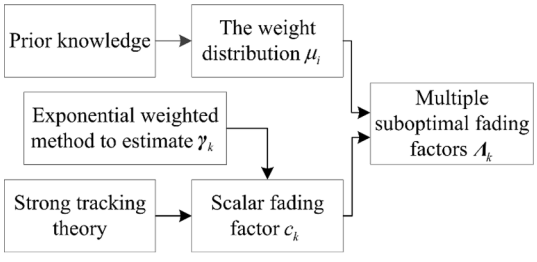

Fig. 1. Construction of multiple fading factors.

approximate distribution of MNCM in the variational update process is given by [15]

$$\begin{aligned} ln q^{(i+1)}(\boldsymbol{R}_k) &= -0.5(d+\hat{v}_{k|k-1}+2)ln|\boldsymbol{R}_k| \\ &\quad -0.5\mathrm{tr}[(\boldsymbol{T}_k^{(i)}+\hat{\boldsymbol{V}}_{k|k-1})\boldsymbol{R}_k^{-1}]+C_R \end{aligned} \tag{24}$$

where $q^{(i)}(\cdot)$ represents the approximate probability distribution of $q(\cdot)$ at the *ith* iteration; C_R is a constant; the covariance matrix $\boldsymbol{T}_k^{(i)}$ is defined as

$$\begin{aligned} \boldsymbol{T}_k^{(i)} &= \mathrm{E}^{(i)}[(\boldsymbol{L}_k-\boldsymbol{H}_k\boldsymbol{X}_k)(\boldsymbol{L}_k-\boldsymbol{H}_k\boldsymbol{X}_k)^{\mathrm{T}}] \\ &= (\boldsymbol{L}_k-\boldsymbol{H}_k\hat{\boldsymbol{X}}_k^{(i)})(\boldsymbol{L}_k-\boldsymbol{H}_k\hat{\boldsymbol{X}}_k^{(i)})^{\mathrm{T}}+\boldsymbol{H}_k\boldsymbol{P}_k^{(i)}\boldsymbol{H}_k^{\mathrm{T}} \end{aligned} \tag{25}$$

It is easy to find that the updated $q^{(i+1)}(\boldsymbol{R}_k)$ follows a new inverse Wishart distribution, that is $q^{(i+1)}(\boldsymbol{R}_k)=\mathrm{IW}(\boldsymbol{R}_k|\hat{v}_k^{(i+1)},\hat{\boldsymbol{V}}_k^{(i+1)})$ whose distribution parameters are given by

$$\hat{v}_k^{(i+1)} = \hat{v}_{k|k-1}+1 \tag{26}$$

$$\hat{\boldsymbol{V}}_k^{(i+1)} = \hat{\boldsymbol{V}}_{k|k-1}+\boldsymbol{T}_k^{(i)} \tag{27}$$

Similarly, the logarithmic expression of the approximate distribution of system state in the variational update process is given by [15]

$$\begin{aligned} ln q^{(i+1)}(\boldsymbol{X}_k) &= -0.5\boldsymbol{X}_k^{\mathrm{T}}(\boldsymbol{P}_{k|k-1}^{-1}+\boldsymbol{H}_k^{\mathrm{T}}\mathrm{E}^{(i+1)}[\boldsymbol{R}_k^{-1}]^{-1}\boldsymbol{H}_k)\boldsymbol{X}_k \\ &\quad +\boldsymbol{X}_k^{\mathrm{T}}(\boldsymbol{P}_{k|k-1}^{-1}\hat{\boldsymbol{X}}_{k|k-1}+\boldsymbol{H}_k^{\mathrm{T}}\mathrm{E}^{(i+1)}[\boldsymbol{R}_k^{-1}]^{-1}\boldsymbol{L}_k)+C_X \end{aligned} \tag{28}$$

where $\mathrm{E}^{(i+1)}[\boldsymbol{R}_k^{-1}] = (\hat{v}_k^{(i+1)}-m-1)(\hat{\boldsymbol{V}}_k^{(i+1)})^{-1}$, the modified MNCM is given by

$$\hat{\boldsymbol{R}}_k^{(i+1)} = \left(\mathrm{E}^{(i+1)}[\boldsymbol{R}_k^{-1}]\right)^{-1} = \left(\hat{v}_k^{(i+1)}-m-1\right)^{-1}\hat{\boldsymbol{V}}_k^{(i+1)} \tag{29}$$

The mean vector and covariance matrix of the $i+1th$ iteration are given by

$$\boldsymbol{K}_k^{(i+1)} = \hat{\boldsymbol{P}}_{k|k-1}^{(i+1)}\boldsymbol{H}_k^{\mathrm{T}}\left(\boldsymbol{H}_k\hat{\boldsymbol{P}}_{k|k-1}^{(i+1)}\boldsymbol{H}_k^{\mathrm{T}}+\hat{\boldsymbol{R}}_k^{(i+1)}\right)^{-1} \tag{30}$$

$$\hat{\boldsymbol{X}}_{k|k}^{(i+1)} = \hat{\boldsymbol{X}}_{k|k-1}+\boldsymbol{K}_k^{(i+1)}(\boldsymbol{L}_k-\boldsymbol{H}_k\hat{\boldsymbol{X}}_{k|k-1}) \tag{31}$$

$$\boldsymbol{P}_{k|k}^{(i+1)} = \hat{\boldsymbol{P}}_{k|k-1}^{(i+1)}-\boldsymbol{K}_k^{(i+1)}\boldsymbol{H}_k\hat{\boldsymbol{P}}_{k|k-1}^{(i+1)} \tag{32}$$

Equations (14)-(15) and Equations (26)-(32) together constitute the variational update process of MST-VBAKF algorithm. The Expectation-Maximization (EM) method [37] is used to repeatedly update parameters $\hat{\boldsymbol{R}}_k^{(i+1)}$ and $\hat{\boldsymbol{X}}_{k|k}^{(i+1)}$. The smaller the KL divergence is, the closer the product of $q^{(i+1)}(\boldsymbol{X}_k)$ and $q^{(i+1)}(\boldsymbol{R}_k)$ is to $p(\boldsymbol{X}_k,\boldsymbol{R}_k|\boldsymbol{L}_{1:k})$, and the optimal estimations of $\hat{\boldsymbol{R}}_k^{(i+1)}$ and $\hat{\boldsymbol{X}}_{k|k}^{(i+1)}$ are obtained until the variational update process is completed. The workflow of MST-VBAKF algorithm is shown in Fig. 2, where N represents the number of iterations and K denotes the length of simulation time.

4. The experimental simulation

Like many existing researches [15,18,19], this paper adopts the continuous white noise acceleration model in two-dimensional (2D) Cartesian coordinates to verify the performance of the proposed MST-VBAKF algorithm, where the PNCM and MNCM of the target change slowly with time. It is assumed that the motion process is monitored in real time by sensors such as the global navigation satellite systems (GNSS). The position and velocity of target are respectively denoted as $(x_k,\ y_k)$ and $(\dot{x}_k,\ \dot{y}_k)$, and the state vector is defined as $\boldsymbol{X}_k \triangleq [x_k\ y_k\ \dot{x}_k\ \dot{y}_k]^{\mathrm{T}}$. The time-varying models of true PNCM and MNCM are given by [15,18]:

$$\boldsymbol{Q}_k^{true} = (6.5+0.5cos(\frac{\pi k}{K}))\sigma_w^2\begin{bmatrix} \frac{\Delta t^3}{3}\boldsymbol{I}_2 & \frac{\Delta t^2}{2}\boldsymbol{I}_2 \\ \frac{\Delta t^2}{2}\boldsymbol{I}_2 & \Delta t\boldsymbol{I}_2 \end{bmatrix} \tag{33}$$

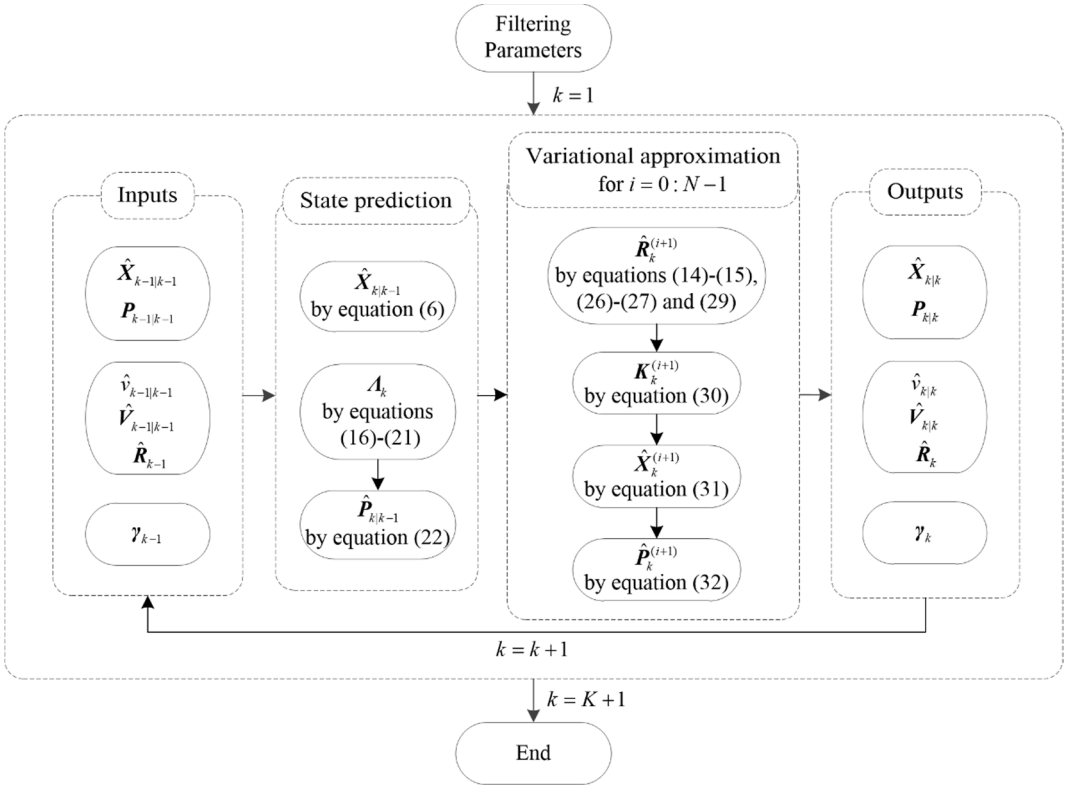

Fig. 2. Flow chart of MST-VBAKF algorithm.

$$\boldsymbol{R}_k^{true} = (0.1 + 0.05cos(\frac{\pi k}{K}))\sigma_v^2 \begin{bmatrix} 1 & 0.5 \\ 0.5 & 1 \end{bmatrix} \tag{34}$$

where $K = 2000$ s is simulation time; $\Delta t = 1$ s is the sampling interval; I represents the identity matrix, whose subscript represents the dimension of the matrix; $\sigma_w^2 = 1\ \mathrm{m}^2/\mathrm{s}^3$ and $\sigma_v^2 = 100\ \mathrm{m}^2$ are noise correlation parameters. In addition, the nominal PNCM and MNCM are respectively set as $\boldsymbol{Q}_k^{\text{nominal}} = \alpha \boldsymbol{I}_4$ and $\boldsymbol{R}_k^{\text{nominal}} = \delta \boldsymbol{I}_4$ in the simulation process, where α and δ are prior confidence parameters, which are used to adjust the initial fixed noise covariance.

Other parameters of MST-VBAKF algorithm are set as follows. The main function of changing factor $\rho \in (0,\ 1]$ is to ensure that the posteriori and prior PDFs have the same forms, which can be set as $\rho = 1 - exp(-4)$ since the noise in the simulation changes slowly [19]. In general, filtering convergence can be achieved by performing the VB approach more than 6 times, thus the number of variational iterations can be set as $N = 10$ [15]. The nominal PNCM and MNCM in the experimental simulation need to be determined according to the prior information of the system. Note the improper α and δ will lead to the estimation error of the filtering and even the filtering divergence. Therefore, in view of the characteristics of the simulation system, the prior confidence parameters can be set as $\alpha = 1$, $\delta = 100$, respectively [15]. The weakening factor $\beta \in (0,\ 1]$ and forgetting factor $\zeta \in [0.65,\ 0.95]$ are adopted to construct the multiple fading factors [19,26]. When the MNCM is relatively accurate, β can take a larger value; when the MNCM is significantly inaccurate, β can take a smaller value to make the estimation result smoother. The forgetting factor affects the estimation accuracy of the PECM. For the system with relatively gentle interference, a larger ζ is taken; otherwise, a smaller ζ should be taken to ensure the utilization ratio of the innovation sequence.

See Appendix A for the pseudocode of the proposed filtering algorithm. In the simulation process, the KF with true PNCM and MNCM (KFTCM), the KF with nominal PNCM and MNCM (KFNCM) and other filters using nominal noise covariance matrix include VBAKF, N-VBAKF and ST-VBAKF are used to verify the performance of the proposed MST-VBAKF. All algorithms are programmed by MATLAB, in which matrix inversion is replaced by matrix division to improve the operation rate. A computer with Intel Core i5-5200U (2.20 GHz) central process unit is adopted to perform the tests, and its random access memory size is 12.0 GB.

4.1. Analysis on the values of weakening and forgetting factors

In order to explore the appropriate value of the weakening factor β, make the filtering estimation result smoother, and enhance the robustness of the filter, $M = 500$ Monte Carlo simulations are performed to compare the performance of the KFTCM, the KFNCM and the MST-VBAKF when β is set to different values, in which the forgetting factor $\zeta = 0.85$.

The square root of the normalized Frobenius norms (SRNFNs) are selected as the error measures to evaluate the estimation accuracy of PECM and MNCM. The SRNFN of the filtering at time k is defined as [15]:

$$SRNFN_k \triangleq \left(\frac{1}{n^2 M} \sum_{s=1}^{M} \| \widehat{\boldsymbol{A}}_{k|k-1}^s - \boldsymbol{A}_{\mathrm{a},k|k-1}^s \|^2 \right)^{\frac{1}{4}} \tag{35}$$

where $\|\boldsymbol{A}\|^2$ represents the trace of the matrix $\boldsymbol{A}\boldsymbol{A}^{\mathrm{T}}$, which can be obtained by summing the main diagonal elements of $\boldsymbol{A}\boldsymbol{A}^{\mathrm{T}}$; $\widehat{\boldsymbol{A}}_{k|k-1}^s$ denotes the estimated PECM or MNCM for running at *sth* Monte Carlo simulation; $\boldsymbol{A}_{\mathrm{a},k|k-1}^s$ denotes the true PECM or MNCM at *sth* Monte Carlo simulation. The average SRNFN (ASRNFN) of the whole simulation is easily obtained by Equation (35), please refer to [14] for details. The ASRNFNs of the PECM and MNCM are recorded as $ASRNFN_P$ and $ASRNFN_M$, respectively.

The root mean square errors (RMSEs) of position and velocity are selected as the performance indexs to evaluate the filtering state estimation accuracy. The RMSE of the filtering at time k is defined as

$$RMSE_k \triangleq \left(\frac{1}{M} \sum_{s=1}^{M} \left(\left(x_k^s - \widehat{x}_k^s \right)^2 + \left(y_k^s - \widehat{y}_k^s \right)^2 \right) \right)^{\frac{1}{2}} \tag{36}$$

where $(x_k^s,\ y_k^s)$ represents the true position or velocity at *sth* Monte Carlo simulation; $\left(\widehat{x}_k^s,\ \widehat{y}_k^s\right)$ represents the estimated position or velocity at *sth* Monte Carlo simulation. According to Equation (36), it is easy to get the average RMSE (ARMSE) of the whole simulation [15]. The ARMSEs of position and velocity are denoted as $ARMSE_P$ and $ARMSE_V$, respectively.

Fig. 3 shows the SRNFNs of PECM and MNCM from KFNCM and MST-VBAKF when $\beta = 0.2,\ 0.3,\ 0.4,\ 0.6,\ 0.8,\ 1.0$. As can be seen from Fig. 3, the overall performance of $SRNFN_P$ from KFNCM shows an increasing trend, while the overall performance of $SRNFN_P$ from MST-VBAKF shows a decreasing trend, and the $SRNFN_P$ from MST-VBAKF is lower than that from KFNCM after the 50 s. The changes of $ASRNFN_P$ from MST-VBAKF when $\beta = 0.2,\ 0.3,\ 0.4,\ 0.6,\ 0.8,\ 1.0$ respectively are not obvious, but the $ASRNFN_P$ increases with the decrease of β. In the whole simulation process, the $SRNFN_M$ from MST-VBAKF is obviously lower than that from KFNCM. The smaller the β is, the smaller the $ASRNFN_M$ from MST-VBAKF is and the faster the convergence speed is. When $\beta = 0.3$, $ASRNFN_M$ from MST-VBAKF is the smallest. Obviously, the change of β has the opposite effect on the $ASRNFN_P$ and $ASRNFN_M$ from MST-VBAKF. This is because the variational Bayesian updated MNCM is adopted to construct multiple fading factors, which is a more accurate estimation for MST-VBAKF algorithm, but inaccurate prior information will be introduced into PECM due to the smaller β.

Fig. 4 shows the RMSEs of position and velocity from KFTCM, KFNCM and MST-VBAKF when $\beta = 0.2,\ 0.3,\ 0.4,\ 0.6,\ 0.8,\ 1.0$. It can be seen from Fig. 4 that the $RMSE_P$ from MST-VBAKF is significantly smaller than that from KFNCM. When β gradually decreases, the $ARMSE_P$ from MST-VBAKF first decreases and then increases, and is closest to that from KFTCM at $\beta = 0.4$. Being similar with $ARMSE_P$, the $ARMSE_V$ from MST-VBAKF is less than that from KFNCM. However, when β gradually decreases, the $ARMSE_V$ from MST-VBAKF shows a decreasing trend in a small range and is the smallest at $\beta = 0.3$. In general, too large or too small β will reduce the state estimation accuracy of MST-VBAKF. Compared with position components, velocity

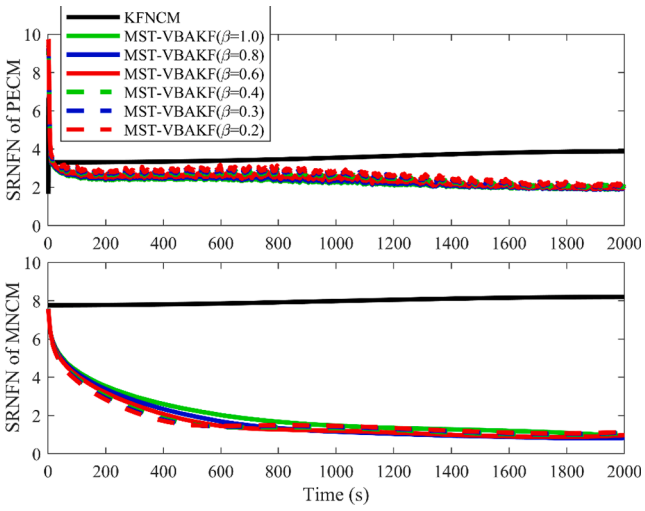

Fig. 3. SRNFNs of PECM and MNCM from KFNCM and MST-VBAKF when $\beta = 0.2,\ 0.3,\ 0.4,\ 0.6,\ 0.8,\ 1.0$.

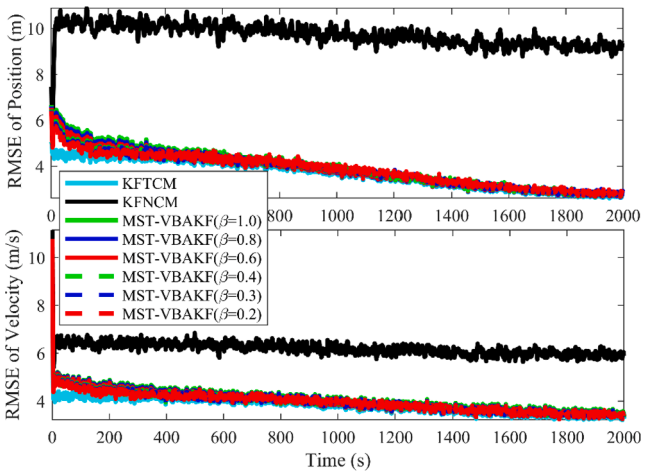

Fig. 4. RMSEs of the position and velocity from KFTCM, KFNCM and MST-VBAKF when $\beta = 0.2, 0.3, 0.4, 0.6, 0.8, 1.0$.

components are less affected by β since their corresponding fading factors are given greater weights.

In order to explore the influence of forgetting factor ζ on the filtering performance, KFNCM, KFTCM and MST-VBAKF with different ζ are tested separately in the $M = 500$ Monte Carlo simulations, where the weakening factor $\beta = 0.4$. Fig. 5 shows the SRNFNs of PECM and MNCM from KFNCM and MST-VBAKF when $\zeta = 0.65, 0.75, 0.85, 0.95$. It can be seen from Fig. 5 that, compared with KFNCM, the MST-VBAKF has obvious advantages in regulating the SRNFN of PECM and can effectively reduce $ASRNFN_P$. When ζ increases, the $ASRNFN_P$ from MST-VBAKF gradually decreases in a relatively significant way. Because the system noise changes gently in the simulation, setting ζ as a larger value can augment the utilization ratio of historical residual data, thus improve the estimation accuracy of PECM. However, the $ASRNFN_M$ of MST-VBAKF increases gradually in a small range with ζ increase, which indicates that the value of ζ has completely opposite influence on PECM and MNCM. Compared with MNCM, the value of ζ has a greater impact on the estimation accuracy of PECM.

Fig. 6 shows the RMSEs of position and velocity from KFTCM, KFNCM and MST-VBAKF when $\zeta = 0.65, 0.75, 0.85, 0.95$. As can be seen from Fig. 6, both in terms of position and velocity, the MST-VBAKF has higher estimation accuracy as compared with KFNCM. When ζ increases, $ARMSE_P$ and $ARMSE_V$ of MST-VBAKF decrease, and the filtering convergence speed slows down to different degrees. However, it is more

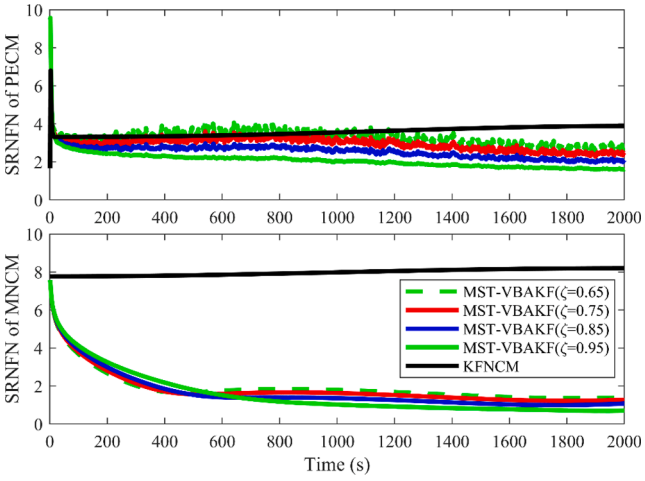

Fig. 5. SRNFNs of the PECM and MNCM from KFNCM and MST-VBAKF when $\zeta = 0.65, 0.75, 0.85, 0.95$.

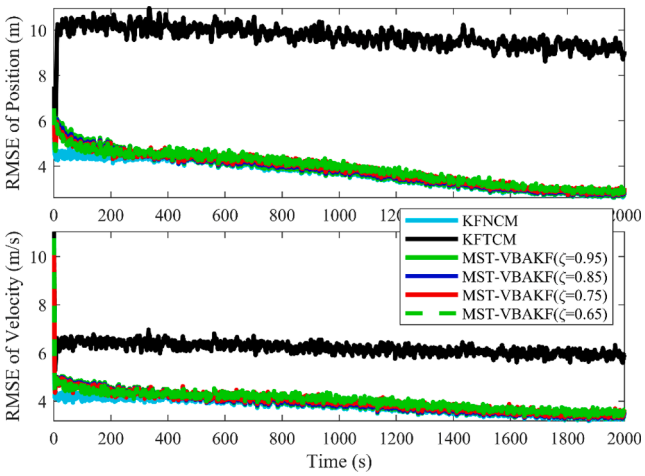

Fig. 6. RMSEs of the position and velocity from KFTCM, KFNCM and MST-VBAKF when $\zeta = 0.65, 0.75, 0.85, 0.95$.

important to reduce the ARMSE of the filtering state vector estimation than to speed up the filtering convergence, hence it can be considered to set ζ as a larger value in simulations of the following study.

4.2. Robustness analysis for initial setting of nominal noise covariance matrix

In some applications, the prior confidence parameters may not be $\alpha = 1$ and $\delta = 100$, that is, the setting of nominal noise covariance matrix is different from that in this paper. In order to verify the adaptive correction capability of MST-VBAKF for nominal process and noise covariance matrix when α and δ are taken as different values, a total of 52×52 combinations are simulated when $\alpha \in [0.1, 500]$ and $\delta \in [0.1, 500]$. The weakening factor β and forgetting factor ζ are set as 0.4 and 0.85, respectively. Considering the time-consuming problem of simulation and ensuring the persuasive result of simulation, the number of Monte Carlo simulations is set as $M = 20$. Fig. 7 shows the ARMSEs of estimated position and velocity from MST-VBAKF.

As can be seen from Fig. 7, the ARMSEs of position and velocity are relatively stable when $\alpha \in [50, 500]$ and $\delta \in [50, 500]$, and the estimated results of position and velocity are closer to the real value. For the ARMSEs of the estimated position, when $\alpha \in [0.1, 50)$ and $\delta \in [50, 500]$, the $ARMSE_P$ decreases first and then increases with decrease of α in the simulations under different δ, and the minimum value and maximum value are obtained approximately at $\alpha = 10$ and $\alpha = 0.1$,

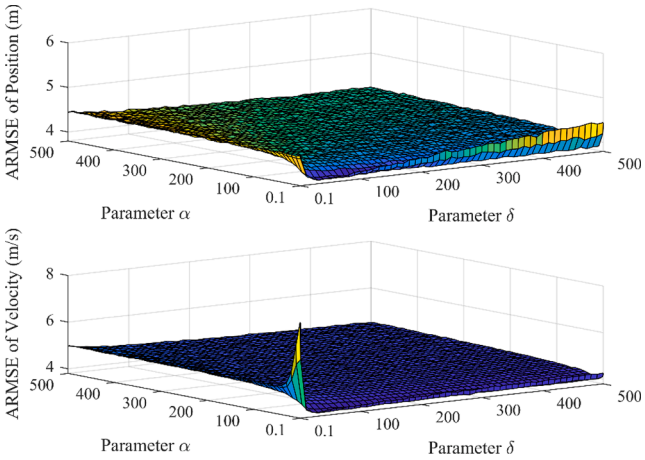

Fig. 7. The ARMSEs of the position and the velocity when α and δ are set as different values

respectively; When $\alpha \in [50,\ 500]$ and $\delta \in [0.1,\ 50)$, the $ARMSE_P$ increases monotonously with decrease of δ in the simulations under different α, and get the maximum value at $\delta = 0.1$ approximately. The ARMSEs of estimated velocities vary in a manner similar to that of positions when α and δ are taken as different values. When $\alpha = 0.1$ and $\delta = 0.1$, because the nominal error covariance matrix setting seriously deviates from the real error covariance matrix, the ARMSEs of positions and velocities both have great estimation errors, and the filtering performance is reduced. The simulation results also show that the variational Bayesian method can only ensure local convergence. In general, for the value of large parts of α and δ, the estimation results of MST-VBAKF algorithm can converge to the stable value, and reflect good robustness of estimation.

4.3. Comparison with advanced filtering algorithms

In order to compare the performance of the proposed method with that of the advanced filtering algorithms, the KFTCM, the KFNCM, the VBAKF, the N-VBAKF, the ST-VBAKF and the MST-VBAKF are tested respectively in $M = 500$ Monte Carlo simulations. The weakening factor and forgetting factor are set as $\beta = 0.4$ and $\zeta = 0.85$, respectively. Fig. 8 shows the SRNFNs of PECM and MNCM from different filtering algorithms, and it can be seen from Fig. 8 that the KFNCM has the lowest accuracy due to the lack of real-time estimation and update capability for PECM and MNCM. The convergence speed of VBAKF is slow, and the SRNFN of MNCM from VBAKF is smaller than that from KFTCM after about 730 s. The errors are introduced into the variational update process of MNCM since VBAKF lacks the ability to update PECM. The estimation accuracy of MNCM from ST-VBAKF using single fading factor is barely better than that of N-VBAKF, but the estimation accuracy of PECM from ST-VBAKF is worse. Compared with the ST-VBAKF, the MST-VBAKF overcomes the limitation of poor tracking ability of single fading factor for multiple variables and has higher estimation accuracy for time-varying PECM and MNCM. Table 1 lists the ASRNFNs of PECM and MNCM from each filtering algorithm. It can be seen from Table 1 that compared with the VBAKF method, the $ASRNFN_P$ of PECM and the $ASRNFN_M$ of MNCM from MST-VBAKF are improved by 16.3% and 66.3%, respectively.

Fig. 9 shows the RMSEs of position and velocity from different filtering algorithms. It can be seen from Fig. 9 that compared with other algorithms, the convergence speed of MST-VBAKF for position or velocity is closer to KFTCM. In addition, the $ARMSE_P$ and the $ARMSE_V$ are also the smallest because the MST-VBAKF has the highest estimation accuracy for PECM and MNCM. Table 2 lists the ARMSEs of position and velocity from each filtering algorithm. It can be seen from Table 2 that MST-VBAKF has the highest estimation accuracy of state vector among the six filtering algorithms. Compared with VBAKF, the $ARMSE_P$ and the $ARMSE_V$ from MST-VBAKF are improved by 57.1% and 32.6%, respectively. To summarise, the proposed MST-VBAKF algorithm can estimate PECM and MNCM more accurately and has a higher estimation accuracy for state vector as compared with existing filters.

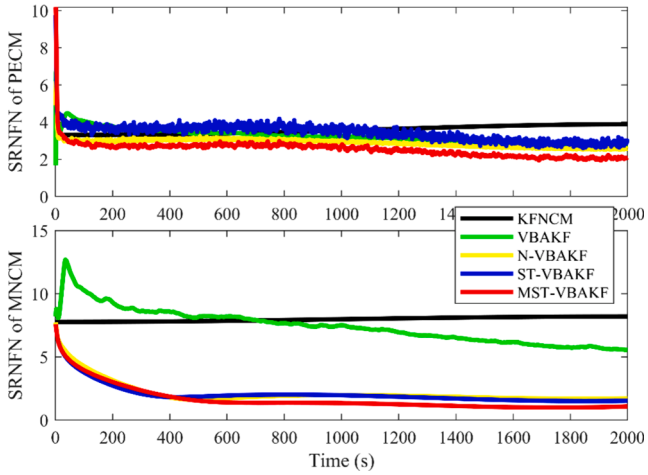

Fig. 8. SRNFNs of the PECM and MNCM from different filtering algorithms

Table 1
The ASRNFNs of PECM and MNCM from different filtering algorithms.

Algorithm type	$ASRNFN_P$	$ASRNFN_M$
KFTCM	/	/
KFNCM	3.61	7.99
VBAKF	3.31	7.84
N-VBAKF	2.92	2.86
ST-VBAKF	3.53	2.67
MST-VBAKF	2.77	2.64

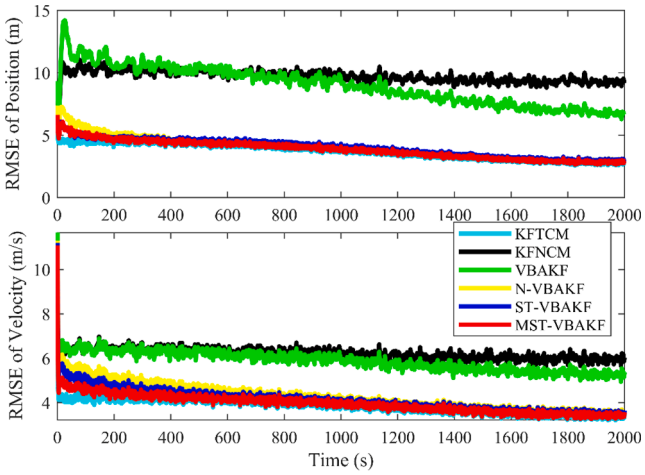

Fig. 9. RMSEs of the position and velocity from different filtering algorithms

Table 2
The ARMSEs of position and velocity from different filtering algorithms.

Algorithm type	$ARMSE_P$ (m)	$ARMSE_V$ (m/s)
KFTCM	3.75	3.85
KFNCM	9.74	6.20
VBAKF	9.12	5.89
N-VBAKF	4.12	4.31
ST-VBAKF	4.04	4.14
MST-VBAKF	3.91	3.97

5. Conclusions

When the PNCM and MNCM of the dynamic system are time-varying, the KF is not ideal for parameter estimation accuracy, while existing filter algorithms are not able to weaken the influence of inaccurate PNCM on filtering performance or have limited ability to weaken. On the basis of existing researches, this paper proposes a strong tracking variational Bayesian adaptive filtering algorithm with multiple fading factors, namely MST-VBAKF, which can adjust the PECM and MNCM simultaneously. Simulation results show that the proposed filtering algorithm has a higher estimation accuracy for state vector compared with existing filters, and its features are analyzed as follows: 1) Inverse Wishart distribution is used to more accurately describe the inaccurate noise model and obtain the local optimal estimation of MNCM and state vector through the VB approach; 2) Since the updated MNCM and the innovation covariance matrix estimated based on the fading memory exponential weighting method are adopted to calculate multiple fading factors, the estimation accuracy of PECM is significantly improved.

CRediT authorship contribution statement

Cheng Pan: Conceptualization, Methodology, Formal analysis, Writing - original draft. **Jingxiang Gao:** Supervision, Project administration, Funding acquisition. **Zengke Li:** Software, Visualization. **Nijia Qian:** Investigation, Writing - review & editing. **Fangchao Li:** Investigation, Writing - review & editing.

Declaration of Competing Interest

The authors declare that they have no known competing financial interests or personal relationships that could have appeared to influence the work reported in this paper.

Acknowledgements

This work is supported by the National Natural Science Foundation of China (grant numbers 41974026, 41874006), the China University of Mining and Technology (grant number 2020WLJCRCZL052), and the Jiangsu Education Department (grant number KYCX20_2058). The authors are grateful for the three anonymous reviewers for their constructive comments on the manuscript.

Appendix A. The pseudocode of the proposed MST-VBAKF at time k

Inputs: $\widehat{\boldsymbol{X}}_{k-1|k-1}$, $\boldsymbol{P}_{k-1|k-1}$, $\widehat{\nu}_{k-1|k-1}$, $\widehat{\boldsymbol{V}}_{k-1|k-1}$, $\boldsymbol{F}_{k-1}$, $\boldsymbol{H}_k$, $\boldsymbol{L}_k$, $\boldsymbol{Q}_{k-1}$, $\boldsymbol{\mu}$, m, n, ζ, β, N, ρ

Time update:

1: $\widehat{\boldsymbol{X}}_{k|k-1} = \boldsymbol{F}_{k-1}\widehat{\boldsymbol{X}}_{k-1|k-1}$, $\boldsymbol{\xi}_k = \boldsymbol{L}_k - \boldsymbol{H}_k\widehat{\boldsymbol{X}}_{k|k-1}$

Multiple suboptimal fading factors are introduced:

2: $\gamma_k = \dfrac{(1-\zeta)\boldsymbol{\xi}_k\boldsymbol{\xi}_k^{\mathrm{T}} + (\zeta-\zeta^k)\gamma_{k-1}}{1-\zeta^k}$, $\gamma_0 = 0$

3: $\boldsymbol{N}_k = \gamma_k - \boldsymbol{H}_k\boldsymbol{Q}_{k-1}\boldsymbol{H}_k^{\mathrm{T}} - \beta\widehat{\boldsymbol{R}}_k$

4: $\boldsymbol{M}_k = \boldsymbol{H}_k\boldsymbol{F}_{k-1}\boldsymbol{P}_{k-1|k-1}\boldsymbol{F}_{k-1}^{\mathrm{T}}\boldsymbol{H}_k^{\mathrm{T}}$

5: $c_k = \begin{cases} \widetilde{c}, & \widetilde{c} > 1 \\ 1, & \widetilde{c} \leqslant 1 \end{cases}$, $\widetilde{c} = \mathrm{tr}[\boldsymbol{N}_k]/\sum_{i=1}^{d}\mu_i\boldsymbol{M}_k^{ii}$

6: $\lambda_{i,k} = \mu_i c_k$, $i = 1, \cdots, \boldsymbol{n}$

7: $\boldsymbol{\Lambda}_k = \mathrm{diag}\left(\lambda_{1,k}, \lambda_{2,k}, \ldots, \lambda_{n,k}\right)$

8: $\widehat{\boldsymbol{P}}_{k|k-1} = \boldsymbol{\Lambda}_k\boldsymbol{F}_{k-1}\boldsymbol{P}_{k-1}\boldsymbol{F}_{k|k-1}^{\mathrm{T}} + \widetilde{\boldsymbol{Q}}_{k-1}$

Variational measurement update:

9: Initialization: $\widehat{\boldsymbol{X}}_{k|k}^{(0)} = \widehat{\boldsymbol{X}}_{k|k-1}$, $\boldsymbol{P}_{k|k}^{(0)} = \boldsymbol{P}_{k|k-1}$, $\widehat{\boldsymbol{V}}_{k|k-1} = \rho\widehat{\boldsymbol{V}}_{k-1|k-1}$, $\widehat{\nu}_{k|k-1} = \rho\left(\widehat{\nu}_{k-1|k-1} - m - 1\right) + m + 1$

for $i = 0 : N-1$

10: $\boldsymbol{T}_k^{(i)} = \left(\boldsymbol{L}_k - \boldsymbol{H}_k\widehat{\boldsymbol{X}}_{k|k}^{(i)}\right)\left(\boldsymbol{L}_k - \boldsymbol{H}_k\widehat{\boldsymbol{X}}_{k|k}^{(i)}\right)^{\mathrm{T}} + \boldsymbol{H}_k\boldsymbol{P}_{k|k}^{(i)}\boldsymbol{H}_k^{\mathrm{T}}$

11: $\widehat{\nu}_k^{(i+1)} = \widehat{\nu}_{k|k-1} + 1$, $\widehat{\boldsymbol{V}}_k^{(i+1)} = \widehat{\boldsymbol{V}}_{k|k-1} + \boldsymbol{T}_k^{(i)}$

12: $\widehat{\boldsymbol{R}}_k^{(i+1)} = \left(\widehat{\nu}_k^{(i+1)} - m - 1\right)^{-1}\widehat{\boldsymbol{V}}_k^{(i+1)}$

13: $\boldsymbol{K}_k^{(i+1)} = \widehat{\boldsymbol{P}}_{k|k-1}^{(i+1)}\boldsymbol{H}_k^{\mathrm{T}}\left(\boldsymbol{H}_k\widehat{\boldsymbol{P}}_{k|k-1}^{(i+1)}\boldsymbol{H}_k^{\mathrm{T}} + \widehat{\boldsymbol{R}}_k^{(i+1)}\right)^{-1}$

14: $\widehat{\boldsymbol{X}}_{k|k}^{(i+1)} = \widehat{\boldsymbol{X}}_{k|k-1} + \boldsymbol{K}_k^{(i+1)}\left(\boldsymbol{L}_k - \boldsymbol{H}_k\widehat{\boldsymbol{X}}_{k|k-1}\right)$

15: $\boldsymbol{P}_{k|k}^{(i+1)} = \widehat{\boldsymbol{P}}_{k|k-1}^{(i+1)} - \boldsymbol{K}_k^{(i+1)}\boldsymbol{H}_k\widehat{\boldsymbol{P}}_{k|k-1}^{(i+1)}$

end for

16: $\widehat{\boldsymbol{X}}_{k|k} = \widehat{\boldsymbol{X}}_{k|k}^{(N)}$, $\boldsymbol{P}_{k|k} = \boldsymbol{P}_{k|k}^{(N)}$, $\widehat{\nu}_{k|k} = \widehat{\nu}_k^{(N)}$, $\widehat{\boldsymbol{V}}_{k|k} = \widehat{\boldsymbol{V}}_k^{(N)}$, $\widehat{\boldsymbol{R}}_{k|k} = \widehat{\boldsymbol{R}}_k^N$

Outputs: $\widehat{\boldsymbol{X}}_{k|k}$, $\boldsymbol{P}_{k|k}$, $\widehat{\nu}_{k|k}$, $\widehat{\boldsymbol{V}}_{k|k}$, $\widehat{\boldsymbol{P}}_{k,k-1}$, $\widehat{\boldsymbol{R}}_k$, γ_k

Appendix B. Supplementary material

Supplementary data to this article can be found online at https://doi.org/10.1016/j.measurement.2021.109139.

References

[1] T.J. Lim, Y. Ma, The Kalman filter as the optimal linear minimum mean-squared error multiuser CDMA detector, IEEE Trans. Inf. Theory. 46 (2000) 2561–2566, https://doi.org/10.1109/18.887863.

[2] B. Chen, X. Liu, H. Zhao, J.C. Principe, Maximum correntropy Kalman filter, Automatica 76 (2017) 70–77, https://doi.org/10.1016/j.automatica.2016.10.004.

[3] R. Kleinbauer, Kalman filtering implementation with Matlab, University of Stuttgart, 2004.

[4] S. Mahfouz, F. Mourad-Chehade, P. Honeine, J. Farah, H. Snoussi, Target Tracking Using Machine Learning and Kalman Filter in Wireless Sensor Networks, IEEE Sens. J. 14 (2014) 3715–3725, https://doi.org/10.1109/JSEN.2014.2332098.

[5] Y. Huang, Y. Zhang, B. Xu, Z. Wu, J.A. Chambers, A New Adaptive Extended Kalman Filter for Cooperative Localization, IEEE Trans. Aerosp. Electron. Syst. 54 (2018) 353–368, https://doi.org/10.1109/TAES.2017.2756763.

[6] M.H. Amoozgar, A. Chamseddine, Y. Zhang, Experimental Test of a Two-Stage Kalman Filter for Actuator Fault Detection and Diagnosis of an Unmanned Quadrotor Helicopter, J. Intell. Robot. Syst. 70 (2013) 107–117, https://doi.org/10.1007/s10846-012-9757-7.

[7] M. Fayaz, I. Ullah, D.-H. Kim, Underground risk index assessment and prediction using a simplified hierarchical fuzzy logic model and Kalman filter, Processes. 6 (2018) 103.

[8] C. Pan, Z. Li, J. Gao, F. Li, A Variational Bayesian-Based Robust Adaptive Filtering for Precise Point Positioning Using Undifferenced and Uncombined Observations, Adv. Sp. Res. (2020), https://doi.org/10.1016/j.asr.2020.12.022.

[9] P. Axelsson, U. Orguner, F. Gustafsson, M. Norrlöf, ML Estimation of Process Noise Variance in Dynamic Systems, IFAC Proc. 44 (2011) 5609–5614, https://doi.org/10.3182/20110828-6-IT-1002.00543.

[10] M. Yu, INS/GPS Integration System using Adaptive Filter for Estimating Measurement Noise Variance, IEEE Trans. Aerosp. Electron. Syst. 48 (2012) 1786–1792, https://doi.org/10.1109/TAES.2012.6178100.

[11] J.E. Stellet, F. Straub, J. Schumacher, W. Branz, J.M. Zöllner, Estimating the Process Noise Variance for Vehicle Motion Models, 2015 IEEE 18th Int Conf. Intell. Transp. Syst. (2015) 1512–1519, https://doi.org/10.1109/ITSC.2015.212.

[12] B. Ristic, X. Wang, S. Arulampalam, Target motion analysis with unknown measurement noise variance, 2017 20th Int. Conf. Inf. Fusion (2017) 1–8.

[13] S.S. Hosseini, M.M. Jamali, S. Särkkä, Variational Bayesian adaptation of noise covariances in multiple target tracking problems, Measurement 122 (2018) 14–19, https://doi.org/10.1016/j.measurement.2018.02.055.
[14] M. Liu, Y. Gao, G. Li, X. Guang, S. Li, An Improved Alignment Method for the Strapdown Inertial Navigation System (SINS), Sensors. 16 (2016), https://doi.org/10.3390/S16050621.
[15] Y. Huang, Y. Zhang, Z. Wu, N. Li, J. Chambers, A Novel Adaptive Kalman Filter With Inaccurate Process and Measurement Noise Covariance Matrices, IEEE Trans. Automat. Contr. 63 (2018) 594–601, https://doi.org/10.1109/TAC.2017.2730480.
[16] A.H. Mohamed, K.P. Schwarz, Adaptive Kalman filtering for INS/GPS, J. Geod. 73 (1999) 193–203, https://doi.org/10.1007/s001900050236.
[17] Y. Yang, W. Gao, Comparison of two fading filters and adaptively robust filter, Geomatics Inf. Sci. Wuhan Univ. 10 (2007) 200–203.
[18] T. Ardeshiri, E. Özkan, U. Orguner, F. Gustafsson, Approximate Bayesian Smoothing with Unknown Process and Measurement Noise Covariances, IEEE Signal Process. Lett. 22 (2015) 2450–2454, https://doi.org/10.1109/LSP.2015.2490543.
[19] F. Tan, J. Zhao, Strong tracking based variational Bayesian adaptive Kalman filtering algorithm, Electron. Opt. Control. (2020), 12–16+36.
[20] H. Xue, X. Guo, Z. Zhou, SINS initial alignment method based on adaptive multiple fading factors Kalman filter, Syst. Eng. Electron. 39 (2017) 620–626.
[21] Z. Lai, Y. Lei, S. Zhu, Y.-L. Xu, X.-H. Zhang, S. Krishnaswamy, Moving-window extended Kalman filter for structural damage detection with unknown process and measurement noises, Measurement 88 (2016) 428–440, https://doi.org/10.1016/j.measurement.2016.04.016.
[22] D. Zhou, Y. Xi, Z. Zhang, A Suboptimal Multiple Fading Extended Kalman Filter, Acta Autom. Sin. 17 (1991).
[23] Y. Geng, J. Wang, Adaptive estimation of multiple fading factors in Kalman filter for navigation applications, GPS Solut. 12 (2008) 273–279, https://doi.org/10.1007/s10291-007-0084-6.
[24] W. Gao, L. Miao, M. Ni, Multiple Fading Factors Kalman Filter for SINS Static Alignment Application, Chinese J. Aeronaut. 24 (2011) 476–483, https://doi.org/10.1016/S1000-9361(11)60055-1.
[25] H.E. Soken, C. Hajiyev, Adaptive Unscented Kalman Filter with multiple fading factors for pico satellite attitude estimation, 2009 4th Int. Conf. Recent Adv. Sp. Technol. (2009) 541–546, https://doi.org/10.1109/RAST.2009.5158254.
[26] S. Liu, Fault parameter joint estimation based on multiple fading factors strong tracking nonlinear filter, J. Electron. Meas. Instrum. 33 (2019) 164–170.
[27] Y. Huang, Y. Zhang, P. Shi, Z. Wu, J. Qian, J.A. Chambers, Robust Kalman Filters Based on Gaussian Scale Mixture Distributions With Application to Target Tracking, IEEE Trans. Syst. MAN Cybern. 49 (2019) 2082–2096, https://doi.org/10.1109/TSMC.2017.2778269.
[28] N. Qian, G. Chang, J. Gao, Smoothing for continuous dynamical state space models with sampled system coefficients based on sparse kernel learning, Nonlinear Dyn. 100 (2020) 3597–3610, https://doi.org/10.1007/s11071-020-05698-0.
[29] K. Xiong, C. Wei, H. Zhang, Q-learning for noise covariance adaptation in extended KALMAN filter, Asian J. Control. (2020), https://doi.org/10.1002/asjc.2336.
[30] Y. Yang, W. Gao, An Optimal Adaptive Kalman Filter, J. Geod. 80 (2006) 177–183, https://doi.org/10.1007/s00190-006-0041-0.
[31] Z. Li, J. Gao, J. Wang, Y. Yao, PPP/INS tightly coupled navigation using adaptive federated filter, GPS Solut. 21 (2017) 137–148, https://doi.org/10.1007/s10291-015-0511-z.
[32] M.J. Beal, Variational algorithms for approximate Bayesian inference, University of London London, 2003.
[33] S. S, J. Hartikainen, Variational Bayesian Adaptation of Noise Covariances in Non-Linear Kalman Filtering, ArXiv:1302.0681. (2013). https://arxiv.org/pdf/1302.0681.
[34] C. Jiang, S.-B. Zhang, Q.-Z. Zhang, Adaptive Estimation of Multiple Fading Factors for GPS/INS Integrated Navigation Systems, Sensors. 17 (2017), https://doi.org/10.3390/S17061254.
[35] Y. Yang, T. Xu, An Adaptive Kalman Filter Based on Sage Windowing Weights and Variance Components, J. Navig. 56 (2003) 231–240, https://doi.org/10.1017/S0373463303002248.
[36] D.G. Tzikas, A.C. Likas, N.P. Galatsanos, The variational approximation for Bayesian inference, Signal Process. Mag. IEEE. 25 (2008) 131–146, https://doi.org/10.1109/msp.2008.929620.
[37] A.P. Dempster, N.M. Laird, D.B. Rubin, Maximum likelihood from incomplete data via the EM algorithm, J. Roy. Stat. Soc. Ser. B. 39 (1977) 1–38.